Macromolecules

pubs.acs.org/Macromolecules Article

Synthesis of Novel Alicyclic Poly(thioether sulfone) with High Refractive Index and High Abbe's Number Using 1,4-Dithiin 1,1-Dioxide

Keita Watanabe, Kazushi Enomoto, Takumi Nagasawa, Megumi Matsuda, Hiroshi Katagiri, Seigou Kawaguchi, Shinji Ando, Mitsuru Ueda, and Tomoya Higashihara*

Cite This: *Macromolecules* 2025, 58, 4138–4146 Read Online

ACCESS | Metrics & More | Article Recommendations | Supporting Information

ABSTRACT: A novel alicyclic 1,4-dithiin (DT)-based poly(thioether sulfone) (PTES) was successfully synthesized through the polyaddition reaction of 2,5-bis(sulfanylmethyl)-1,4-dithiane (BMMD) with 1,4-dithiin 1,1-dioxide (DTDO). This is the first study to synthesize and identify DTDO with a boat-shaped conformation, as confirmed by nuclear magnetic resonance spectroscopy and X-ray crystallography. It was found that, in a model reaction, benzyl mercaptan (BM) and novel compound, DTDO, underwent the typical Michael-type addition reaction in the presence of a base. Based on this result, the Michael polyaddition reaction between BMMD and DTDO was performed in the presence of *N*,*N*-diisopropylethylamine in *N*-methyl-2-pyrrolidone. As a result, a high-molar-mass PTES, **Poly(BMMD/DTDO)** (M_w up to 23,900 g/mol), was successfully obtained. **Poly(BMMD/DTDO)** features high thermal stability as an aliphatic polymer, exhibiting a 5% weight loss temperature ($T_d^{5\%}$) of 278 °C and a high glass transition temperature (T_g) of 131 °C. The **Poly(BMMD/DTDO)** film exhibited excellent optical properties, including high transparency ($T\%$ = 94.7%@450 nm), average refractive index (n_{av} = 1.6719@594 nm), and Abbe's numbers (ν_d^{TE}/ν_d^{TM} = 37.8/37.6), as predicted by density functional theory calculations. Furthermore, the **Poly(BMMD/DTDO)** film consists of highly isotropic amorphous phases, exhibiting a small birefringence (Δn = −0.0002). The high proportion of alicyclic structures and sulfur content (53.3 wt %), as well as the incorporation of SO_2 units into the polymer, represent a promising molecular design strategy for producing PTESs with excellent thermal and optical properties that are suitable for optical lens materials.

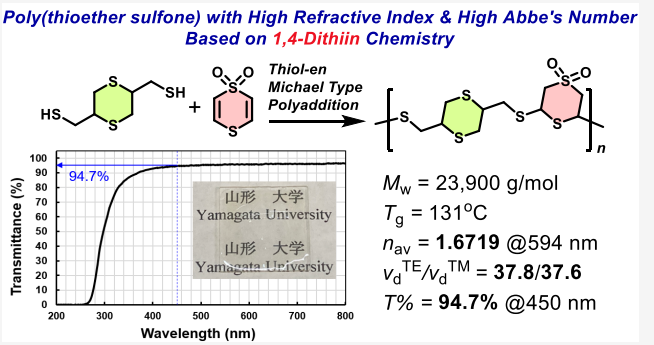

INTRODUCTION

High refractive index (high n) polymers have garnered considerable attention owing to their versatile applications, including in eyeglass/camera lenses, complementary metal−oxide−semiconductor image sensors, antireflective coatings, microlens arrays of organic light-emitting diode devices, touch panels, and optical waveguides.[1−14] High-n polymers can be classified as thermosetting or thermoplastic materials, such as polythiourethanes[15−17] and polycarbonates,[18] respectively. Recently, polymer composite films with inorganic nanofillers have been employed to develop high-n organic−inorganic hybrid materials.[19−24] The refractive index of a material is expressed by the following Lorentz−Lorenz equation

$$\frac{n^2-1}{n^2+2}=\frac{4\pi}{3}\frac{\rho N_A}{M}\alpha=\frac{[R]}{V_0} \quad (1)$$

where n is the refractive index, ρ is the density, N_A is the Avogadro number, M is the molar mass, α is the linear molecular polarizability, $[R]$ is the molar refraction, and V_0 is the molar volume of the polymer repeating unit. Solving this equation for n yields

$$n=\sqrt{\frac{1+2[R]/V_0}{1-[R]/V_0}} \quad (2)$$

Meanwhile, the Abbe's number (ν) is an essential parameter of the wavelength dependence of the refractive index and is approximated as follows

$$\nu_D=\frac{6n_D}{(n_D^2+2)(n_D+1)}\frac{[R]}{[\Delta R]} \quad (3)$$

Received: March 13, 2025
Accepted: April 6, 2025
Published: April 11, 2025

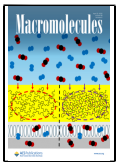

where n_D is the n at the wavelengths of the sodium D line (589.3 nm) and $[\Delta R]$ is the molar dispersion.

n can be effectively increased by introducing nonfluorine halogen atoms, sulfur atoms, or aromatic rings with high $[R]$ values into the polymer chains. However, high $[R]$ and low $[\Delta R]$ values are required to increase ν. For example, aliphatic $-CH_2-$ ($[\Delta R]$ = 0.072)[25] and O═S═O ($[\Delta R]$ = 0.09)[26] units possess low $[\Delta R]$ values, making them preferable for designing high-ν polymers. However, as shown in eq 3, there is a notable trade-off between n and ν values.

For example, Ueda et al. reported the synthesis and optical characterization of soluble thianthrene-based poly(phenylene sulfide)s, showing an average refractive index (n_{av}) of 1.8020 (at 633 nm).[27] Ohishi et al. reported the synthesis and characterization of cyanuric polyimines with polycyclic aromatic hydrocarbon pendants, which exhibited high average n_D (n_D^{av}) values of 1.709−1.800 with ν values at the D line (ν_D) (589 nm) in the range of 11−23.[28] Oyaizu et al. reported the development of a polyphenylene sulfide with a high n_D^{av} value of 1.73−1.85, with the ν_D value varying in the range of 13−25.[29−32] In particular, the ν value tends to rapidly decrease as more aromatic rings are introduced at a monomer repeating unit.

Alicyclic poly(thioether)s (PTEs) are well-known as high-n and high-ν materials.[26,33,34] For example, thermoplastic poly(thioether sulfone)s (PTESs) have been developed by introducing sulfide, sulfone, and alicyclic units into the polymer chains. PTESs were prepared by the Michael polyaddition of 2,5-bis(mercaptomethyl)-1,4-dithiane (BMMD) with divinyl sulfone (DVS) or bis(vinylsulfonyl)-methane (BVSM).[33] Poly(BMMD/DVS) and poly(BMMD/BVSM) exhibited high-n values of 1.6512 and 1.6461, and high-ν values of 42.6 and 43.1, respectively. However, their low glass transition temperatures (T_gs) below 60 °C are unsuitable for lens applications. In general, a T_g value above 100 °C is required for the injection-molding process in optical applications (e.g., poly(methyl methacrylate) (atactic), 105 °C; polycarbonate, 147 °C).[35] The improvement in T_g was accomplished by introducing rigid structures comprising polycyclic hydrocarbons such as tricyclo[5.2.1.02,6]decane, which features three condensed cyclopentanes, in the main chains of PTESs.[34] This led to a considerable improvement in the T_g (up to 113 °C), with an n value of 1.6228 and a high-ν value of 45.8. Although incorporating polycyclic hydrocarbons results in high T_g and ν values, it tends to lower the n value. Therefore, simultaneously achieving high-n, ν, and T_g values remains challenging.

1,4-Dithiin (DT) and its derivatives are interesting motifs for designing PTEs with high-n, ν, and T_g values. DT possesses two reactive double bonds, a high sulfur content (>55 wt %), and a cyclic structure with a boat-shaped six-membered ring.[36] In addition, dioxide and tetraoxide compounds can be synthesized stepwise by oxidizing DT with hydrogen peroxide.[37] Therefore, ν values can be increased by tuning the number of sulfone groups with low $[\Delta R]$. Moreover, the proportion of alicyclic structures of the resulting polymer, which can be obtained via polyaddition between DT derivatives and alicyclic dithiol monomers such as BMMD, becomes higher than those of the polymers obtained using acyclic DVS or BVSM.

Owing to their high chemical stability, thianthrene derivatives comprising the DT skeleton have often been employed to achieve high-n PTEs.[27,38] Conversely, polymers with DT units, which are not stabilized by fused aromatic rings, have rarely been reported. Peng et al. reported the synthesis and optical characterization of poly(DT)s via KOH-assisted polyaddition of elemental sulfur and alkynones;[39] however, the synthesis of PTESs using DT derivatives as monomers has not yet been reported. Therefore, the optical properties of DT-based PTESs are still unknown.

Herein, we designed and synthesized novel DT-based PTESs through the polyaddition of alicyclic BMMD with 1,4-dithiin 1,1-dioxide (DTDO). Obtaining a high proportion of alicyclic structures while maintaining a high sulfur content and tuning the number of SO_2 units is a promising molecular design strategy for producing PTESs with high n (by high sulfur content), high ν (by alicyclic/SO_2 units), low birefringence (Δn) (by small polarizability anisotropy with free rotation around S−C bonds), and moderate T_g (by high density of alicyclic units). These PTESs would be suitable for optical lens materials. To the best of our knowledge, this is the first study to report the synthesis and characterization of DT-based PTESs.

RESULTS AND DISCUSSION

Synthesis of Monomers. Scheme 1 shows the synthetic routes of DTDO, modified from previously reported

Scheme 1. Synthetic Routes of DTDO

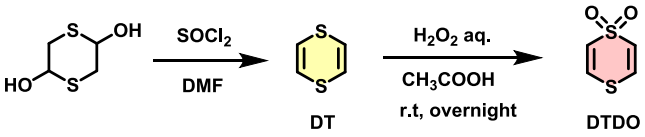

protocols.[37,40] In the first step, DT was obtained in 33% yield by reacting 1,4-dithiane-2,5-diol with thionyl chloride in *N*,*N*-dimethylformamide (DMF), followed by distillation, as confirmed by ^{1}H nuclear magnetic resonance (NMR) (Figure S1a) and ^{13}C NMR (Figure S2). In the second step, DTDO was successfully synthesized in 57% yield *via* the chemoselective oxidation of DT with an excessive H_2O_2 relative to DT at room temperature in acetic acid. The high purity of DTDO, free of byproducts, was confirmed by the ^{1}H NMR (Figure S1b) and ^{13}C NMR spectra (Figure S3). Although the oxidation reaction of DT with H_2O_2 has been previously reported,[37] the chemical structure of the product has not been clearly identified, and only a possibility of DTDO or its regioisomer, 1,4-dithiin 1,4-dioxide, was presented. Therefore, this is the first study to successfully synthesize and identify DTDO. Figure S4 depicts the FT-IR spectrum of DTDO, wherein two sharp peaks are evident at 1265 and 1102 cm^{-1}, corresponding to the O═S═O stretching vibration, and a single sharp peak around 1571 cm^{-1}, assignable to the C═C stretching vibration. The detected absorption peaks are in accordance with those obtained *via* density functional theory (DFT) calculations (Figure S5). A previous study reported the molecular conformations of DT and DTDO as boat and coplanar structures based on DFT calculations, respectively.[41] However, this study found that DTDO also features a boat-shaped conformation similar to DT, as definitively confirmed *via* X-ray crystallography (Figures 1 and S6 and Tables S1 and S2). The asymmetric unit cell contains two independent molecules (Units A and B), and the torsion angles of both clearly indicate the boat conformation of DTDO. To the best of our knowledge, this is the first study to identify the

https://doi.org/10.1021/acs.macromol.5c00676
Macromolecules 2025, 58, 4138−4146

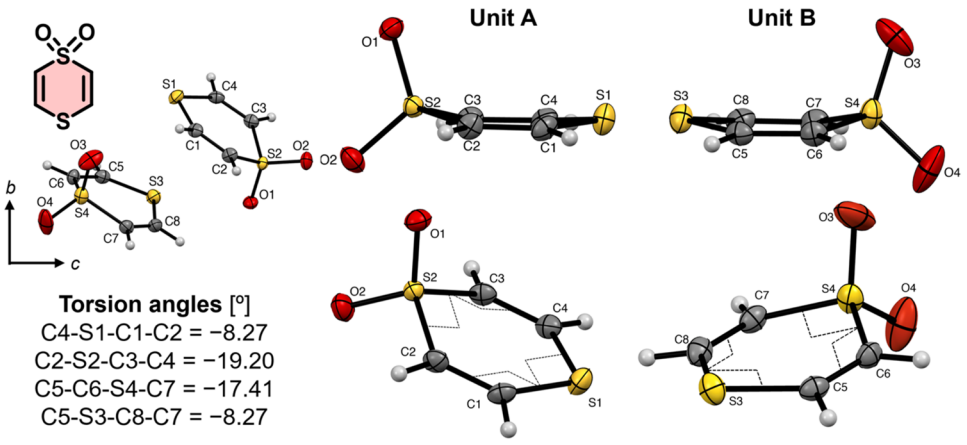

Figure 1. Three-dimensional structures of DTDO obtained *via* X-ray crystallography.

Scheme 2. Model Reaction between BM and DTDO

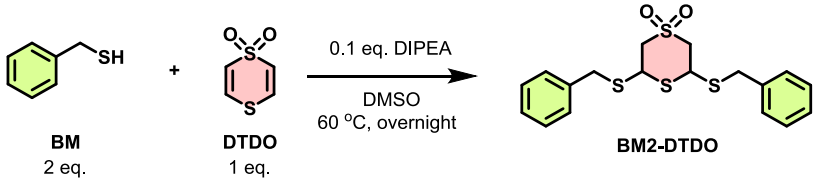

Scheme 3. Synthesis of Poly(BMMD/DTDO)

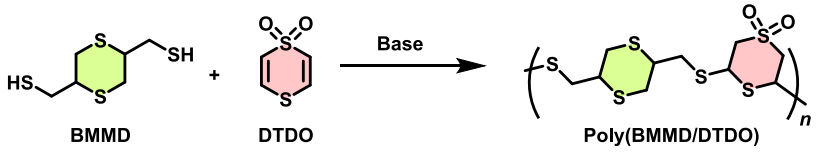

crystalline structure of DTDO in a bulk state. The asymmetric boat conformation of DTDO likely induces a significant dipole moment, potentially leading to the strong absorption of the C═C stretching vibration at 1571 cm^{-1} observed in the FT-IR spectrum.

Model Reaction. Generally, there are two types of well-known thiol−ene reactions; radical and Michael-type addition reactions. Taking into consideration the electron deficiency of vinyl bonds in DTDO originated from the neighbor electron-withdrawing SO_2 groups, we have expected efficient and regioselective Michael-type addition reactions of thiol compounds with DTDO at 3,5-positions corresponding to β carbons. To substantiate this hypothesis, a model reaction of DTDO with benzyl mercaptan (BM) was performed, as shown in Scheme 2. BM was selected as a monothiol reactant as it possesses an aromatic ring that is easily identified in the ^1H NMR spectrum. The model reaction of DTDO with BM was performed in the presence of a catalytic amount of *N*,*N*-diisopropylethylamine (DIPEA). The product, **BM2-DTDO**, was obtained as a white solid in high yield (93%). **BM2-DTDO** was fully characterized by ^1H NMR, $^1H-^1H$ correlation spectroscopy (COSY) NMR, ^{13}C NMR, elemental analysis, and field desorption mass spectroscopy (FD-MS) measurements. In the ^1H NMR spectrum of **BM2-DTDO** (Figure S7), a new characteristic quartet signal ***b*** at 4.5 ppm appeared, assignable to the methine protons (2H). The signals ***c*** (3.9−4.2 ppm) and ***a*** (3.4−3.8 ppm) are assignable to the benzyl methylene protons (4H) and methylene protons next to the SO_2 groups, respectively. The multiplet signals ***d***−***f*** at 7.2−7.4 ppm in the aromatic region are assignable to the aromatic protons (10H). Moreover, in the $^1H-^1H$ COSY NMR spectrum of **BM2-DTDO**, a strong coupling between signals ***a*** and ***b*** can be observed, as expected (Figure S8). The multiplet signals for ***a*** and ***c*** might be the results of the mixture of exo/endo isomers. All these assignments revealed the expected chemical structure of a 3,2/5,6-diadduct compound of DTDO with two equivalents of BM. In the ^{13}C NMR (Figure S9) spectra, the four signals for an aromatic ring and three signals for methine and methylene carbons are evident, assignable to the diadduct compound with 100% regioselectivity at 3-/5-positions. In addition, the values obtained *via* elemental analysis of **BM2-DTDO** (C, 54.78; H, 5.12; S, 32.15) agreed well with the calculated values (C, 54.51; H, 5.08; S, 32.34). Finally, the FD-MS measurements (Figure S10) confirmed that the mass of the diadduct compound (m/z = 396.11) agreed well with the calculated value (m/z = 396.03). Note that the signal at m/z = 792.23, almost double the primary signal, was also observed, corresponding to the dimer of **BM2-DTDO**. We do not have any apparent reason for this contamination at present.

Synthesis of Polymers. Based on the successful model reaction between BM and DTDO based on the Michael-type addition reaction, a novel alicyclic PTES, **Poly(BMMD/DTDO)**, was synthesized by the polyaddition reaction of DTDO with dithiol-based BMMD instead of monothiol-based BM in the presence of bases in dimethyl sulfoxide (DMSO) or *N*-methyl-2-pyrrolidone (NMP), as shown in Scheme 3.

https://doi.org/10.1021/acs.macromol.5c00676
Macromolecules 2025, 58, 4138−4146

Table 1. Polymerization Results of BMMD and DTDO

entry[a]	base type	base (equiv)	temp. (°C)	solvent	time (h)	yield[b] (%)	M_n[c] (g/mol)	M_w[c]	M_w/M_n[c]
1	pyridine	0.1	r.t.	DMSO	3	6	<1220[d]		
2	pyridine	0.1	60	DMSO	22	43	<1220[d]		
3	TEA	0.1	r.t.	DMSO	3	87	<1220[d]		
4	TEA	0.1	60	DMSO	21	98	4810	9230	1.92
5	DIPEA	0.1	60	DMSO	15	93	4870	9400	1.93
6	DIPEA	2.0	60	NMP	22	90	5810	12,800	2.20
7[e]	DIPEA	2.0	60	NMP	17	99	8250[f]	23,900[f]	2.90[f]
8	DIPEA	2.0	80	NMP	24	86	4410	11,200	2.54
9	DBU	0.1	60	NMP	17	89	5080	12,700	2.50
10	DBU	2.0	60	NMP	17	14	1650	4080	2.47

[a]DTDO (0.1 g) was used. [b]Determined by gravimetry after precipitation. [c]Determined by SEC (DMF/LiBr (10 mM), flow rate: 1 mL/min) based on a calibration using polystyrene standards. [d]Less than the minimum M_n of polystyrene standard (M_n = 1220 g/mol) used for calibration in SEC measurement. [e]DTDO monomer (0.3 g) was used. [f]Determined by SEC (*N*-methyl-2-pyrrolidone/LiBr (10 mM), flow rate 0.5 mL/min) based on a calibration using polystyrene standards after purification of the polymer by reprecipitation.

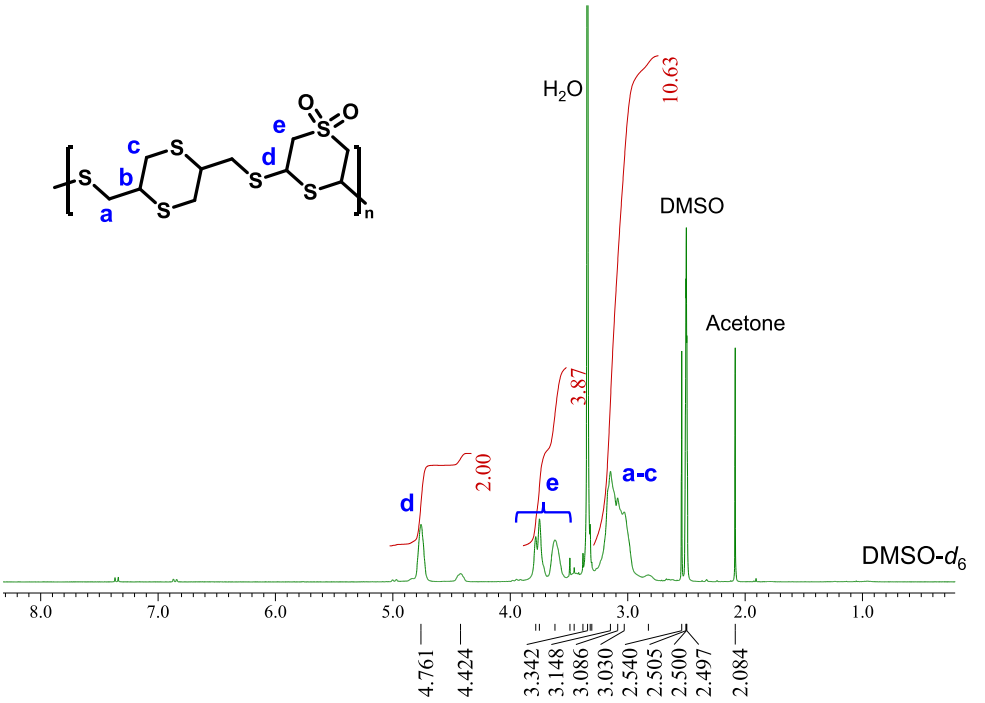

Figure 2. ^{1}H NMR spectrum of **Poly(BMMD/DTDO)** (entry 7).

The experimental results are summarized in Table 1. The polymerization efficiently proceeded when relatively strong bases, such as triethylamine (entry 4), DIPEA, and 1,8-diazabicyclo[5.4.0]-7-undecene (DBU) (entries 5−9), were used, resulting in the formation of the PTES, **Poly(BMMD/DTDO)**, in high yields (86−99%). The use of a large amount of DBU (2.0 equiv. for DTDO) remarkably reduced the polymer yield (14%) due to unwanted side reactions (entry 10). The obtained polymers were characterized via SEC (Figures S11 and S12), ^{1}H NMR (Figure 2), and ^{13}C NMR (Figure S13). **Poly(BMMD/DTDO)** (entry 7) showed the highest M_w value of 23 900 g/mol when DIPEA and NMP were used as the base and solvent, respectively (Table 1 and Figure S12). It was determined that polymerizability depends on the strength of the bases rather than their amounts. In the ^{1}H NMR spectra of **Poly(BMMD/DTDO)** (entry 7), a characteristic peak ***d*** at 4.76 ppm newly appeared, assignable to the methine protons (2H) of thioacetal groups generated by the linkage between BMMD and DTDO units (Figure 2). The signals ***e*** at 3.55−3.8 ppm are attributed to methylene protons (4H) adjacent to sulfone groups in the DTDO units. These multiple signals may originate from the mixture of exo/endo isomers from six-membered rings. In addition, the broad signals at 2.75−3.3 ppm are attributed to the remaining methine and methylene protons (10H) of BMMD units. The expected polymer primary structure was confirmed based on the agreement between the calculated (2:4:10) and observed proton ratios (2:3.87:10.63), as determined through ^{1}H NMR. In addition, ^{1}H−^{1}H COSY NMR spectrum showed the distinct coupling between neighboring protons ***d*** and ***e*** of **Poly(BMMD/DTDO)** (entry 7) (Figure S14), similar to the model compound **BM2-DTDO** (Figure S8), confirming the site selectivity of polymerization at 3-/5-positions of DTDO. The ^{13}C NMR spectrum of **Poly(BMMD/DTDO)** (entry 7)

https://doi.org/10.1021/acs.macromol.5c00676
Macromolecules 2025, 58, 4138−4146

Scheme 4. Plausible Polymerization Mechanism of the Michael-Type Polyaddition Reaction between BMMD and DTDO

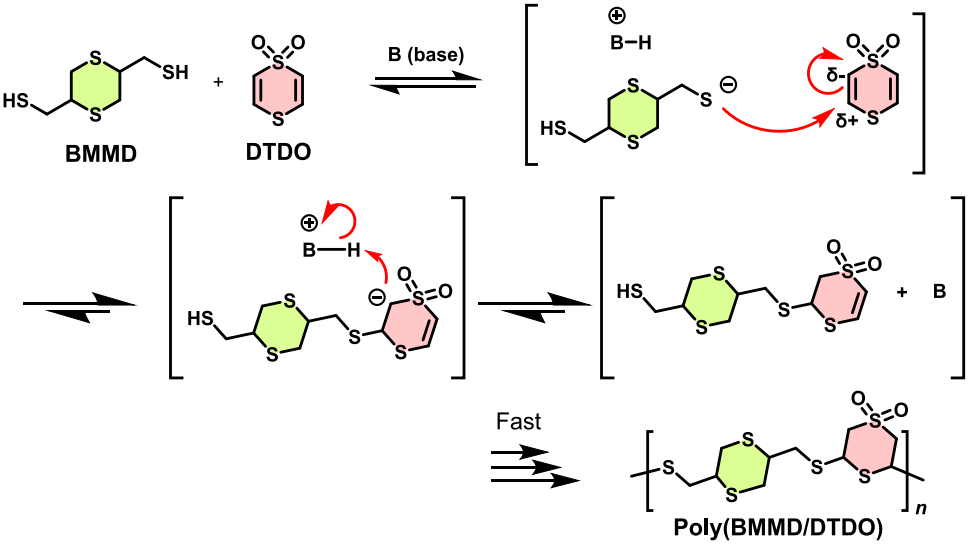

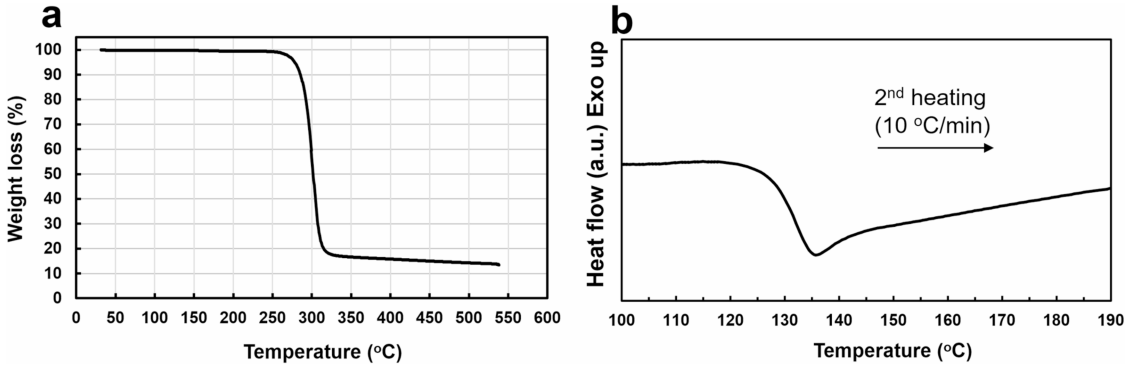

Figure 3. (a) TGA and (b) DSC thermograms of **Poly(BMMD/DTDO)** (entry 7).

showed characteristic signals assignable to five carbons in the monomer repeating units within the aliphatic carbon region of 30−60 ppm (Figure S13). A complex splitting of the carbon signals was observed, again owing to the presence of exo/endo isomers. Thus, the successful synthesis of a novel PTES, **Poly(BMMD/DTDO)**, with high M_w exceeding 20,000 g/mol through an efficient Michael polyaddition reaction was achieved for the first time. This success likely originates from the high reactivity of DTDO with an SO_2 group as an electrophile toward BMMD. Finally, the solubility of **Poly(BMMD/DTDO)** (entry 7) was tested. It was soluble in nonproton polar solvents such as DMSO, *N*,*N*-dimethylacetamide, and NMP; partly soluble in DMF and DMF + LiBr (10 mM); and insoluble in cyclohexanone, chloroform, dichloromethane, tetrahydrofuran, and ethyl acetate at a 1 wt % concentration. The high solubility of **Poly(BMMD/DTDO)** is attributed to the increased polarizability from the incorporation of sulfone groups, as well as the heterogeneity of the mixed exo/endo isomers in the configuration throughout the main chain.

Polymerization Mechanism. Based on the results of the model and polymerization reactions using DTDO with aliphatic thiol compounds, the following mechanism based on the Michael polyaddition reaction is proposed (Scheme 4). During polymerization between DTDO and BMMD, the base can abstract an acidic thiol proton from BMMD to produce a thiolate anion, followed by a Michael addition reaction with an electron-deficient β vinylene carbon of DTDO (3,2-addition) to afford a carbanion intermediate. This carbanion can then abstract a proton from the H-base salt to afford a monoadduct of DTDO with BMMD, thereby regenerating the base. Next, another thiolate anion can react with the remaining β vinylene carbon of the monoadduct compound via the Michael addition reaction (5,6-addition), eventually leading to the polyaddition reactions. Because the polymerization proceeded even using a small amount of base (entry 5), the base likely acts as a catalyst in this system.

A thiol−ene radical addition reaction is an another well-known mechanism and we attempted the polyaddition reaction between DT and BMMD in the presence of azobis(isobutyronitrile) (AIBN); however, only low-molar-mass oligomers or unwanted gels were formed probably by side reactions and/or self-polymerization (see detailed discussions in Supporting Information (SI), Scheme S1, Table S3, and Figures S15−S17).

Thermal Properties. High thermal stability is crucial for manufacturing optical components through injection molding. The thermal properties of **Poly(BMMD/DTDO)** (entry 7) were characterized by thermogravimetric analysis (TGA) and differential scanning calorimetry (DSC) (Figures 3a,b, and S18) and are summarized in Table 2. The $T_d^{5\%}$ value of **Poly(BMMD/DTDO)** (entry 7), determined *via* TGA, was 278 °C, which is comparable to the previously reported value of a similar thioacetal-containing alicyclic PTES.[26] The DSC

https://doi.org/10.1021/acs.macromol.5c00676
Macromolecules 2025, 58, 4138−4146

Table 2. Thermal Properties of the Studied Polymers

polymer	M_w[a] (g/mol)	$T_d^{5\%}$[b] (°C)	T_g[c] (°C)	T_c[c] (°C)	T_m[c] (°C)
poly(BMMD/DTDO)[d]	23,900	278	131		
poly(BMMD/DVS)[25]	26,400[e]	303	47	119	174
poly(BMMD/BVSM)[25]	N/A	278	55		

[a]Determined by SEC based on calibration using polystyrene standards. [b]5 wt % weight loss temperatures determined by TGA. [c]Glass transition temperatures determined by DSC at the second heating scan (10 °C/min). [d]Entry 7. [e]Calculated by the Mn (16,300 g/mol) and M_w/M_n (1.62) values.

thermogram of **Poly(BMMD/DTDO)** (entry 7) showed only T_g and did not reveal any exothermic or endothermic behaviors, indicating its amorphous nature, reflecting isometric conformations of polymers bearing the linkages of mixed endo/exo isomers.[34] The X-ray diffraction pattern of the **Poly(BMMD/DTDO)** (entry 7) film showed only a broad halo, confirming its amorphous nature (Figure S19). The T_g value was significantly improved to 131 °C, compared to those of previously reported aliphatic PTESs employing BMMD (47−55 °C).[33] This likely results from the rigidity of polymer main chains induced by a high density of alicyclic units comprising BMMD and DT-based skeletons, suppressing their micro-Brownian motion. Consequently, introducing highly dense alicyclic units into the polymer main chain, together with sulfone groups, is a promising strategy to enhance the thermal properties of polymers. Notably, the proposed strategy fulfills the requirement of T_g values above 100 °C, indicating that **Poly(BMMD/DTDO)** is well-suited for optical applications employing an injection-molding process.

Optical Properties. The optical properties of **Poly(BMMD/DTDO)** (entry 7) were characterized in the thin-film state, and the results are summarized in Tables 3 and S4. The transmittance of polymer films in the visible region is essential for practical applications of optical engineering materials. The transparency of the **Poly(BMMD/DTDO)** (entry 7) film was evaluated in the 200−800 nm wavelength range via UV−vis spectroscopy (Figure 4). The thin films prepared through the drop-cast method exhibited an excellent transparency of over 94% at 450 nm. This high transparency is attributed to aliphatic structures throughout the main chains and the amorphous nature of the polymers, probably induced by flexible thioether linkages and exo/endo isomers. Figure S20 shows the calculated UV−vis absorption spectra of the model repeating units for **Poly(BMMD/DTDO)**, BMMD/DTDO, compared to those of BMMD/DVS and BMMD/BVSM by TD-DFT. From the result, it is highly expected that all the BMMD-based PTESs show similar cutoff wavelengths at the short wavelength region. Figure S21 shows the experimental UV−vis absorption spectrum of **Poly(BMMD/DTDO)** in DMSO (0.02 mg/mL), also indicating the cutoff wavelength shorter than 350 nm. It was reported that the refractive index dispersion of organic compounds depends on the spectral shape of light absorption, especially near the absorption edges.[26] SO_2 units play an important role in blue-shifted absorption caused by the lowered highest occupied molecular orbital energy level and the increased energy band gap to increase ν values.[26] Figure S22 depicts the calculated wavelength dispersion of n_{av} values of the model repeating units of BMMD/DTDO, BMMD/DVS, and BMMD/BVSM by TD-DFT, indicating that the n_{av} values of BMMD/DTDO are much improved compared to other BMMD-based analogs while minimizing the sacrifice of ν values, probably due to the similar cutoff at the short wavelength region (Figure S20). The highest calculated n_{av} values of BMMD/DTDO are attributable to the highest sulfur content (53.3%) among BMMD-based PTESs.

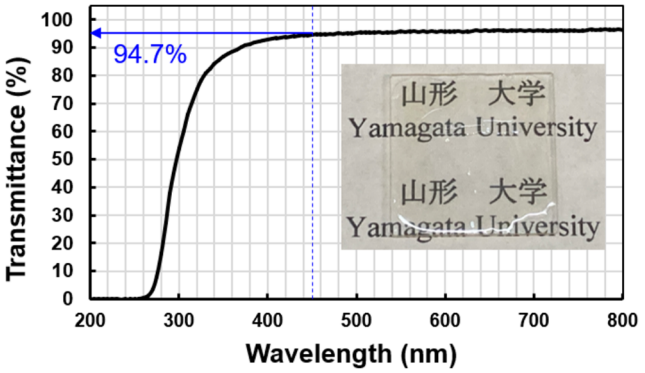

Figure 4. UV−vis transmittance spectrum and photograph of the 12 μm thick **Poly(BMMD/DTDO)** (entry 7) film.

In practice, the refractive indices of the **Poly(BMMD/DTDO)** (entry 7) film were evaluated via a prism coupler method at various wavelengths (473, 594, 636, 653, 845, 1310, and 1558 nm) (Figure 5). The measured n_{av} values almost agree with the expected values based on TD-DFT calculation, being slightly higher than expected at the long wavelength region (Figure S22). The **Poly(BMMD/DTDO)** (entry 7) film showed a high n_{av} value of 1.6719 at 594 nm as well as high ν_d^{TE}/ν_d^{TM} values of 37.8/37.6. Consequently, **Poly(BMMD/DTDO)** exhibits an excellent balance in n_{av} and ν_d values, making it a promising material for manufacturing optical lens materials through injection molding. Table S5 summarizes the measured optical properties of BMMD-based PTESs, indicating the highest n_{av} values of **Poly(BMMD/DTDO)** among all samples, which agreed well with the results from TD-DFT calculation as mentioned above. In addition, the **Poly(BMMD/DTDO)** (entry 7) film also showed a small Δn value of −0.0002, probably owing to the low polarizability

Table 3. Optical Properties of the Poly(BMMD/DTDO) (Entry 7) Film[a]

sulfur content (wt %)			[d]					
calcd	obst[b]	T_{450nm}[c] (%)	n^{TE}[d]	n^{TM}[d]	n_{av}[e]	n[f]	ν_d^{TE}[g]	ν_d^{TM}[g]
53.3	52.6	94.7	1.6718	1.6720	1.6719	−0.0002	37.8	37.6

[a]Film thickness is 8−10 μm. [b]Sulfur contents were measured by elemental analysis. [c]Transmittance of the films at 450 nm. [d]Refractive index values measured using a prism coupler method at 594 nm. The subscripts of TE and TM indicate in-plane and out-of-plane to the substrates, respectively. [e]Averaged refractive index values calculated using the equation $n_{av} = ((2(n_d^{TE})^2 + (n_d^{TM})^2)/3)^{1/2}$. [f]Birefringence was calculated using the equation $\Delta n = n^{TE} - n^{TM}$. [g]Abbe's numbers determined using a prism coupler method. The subscripts of TE and TM indicate in-plane and out-of-plane to the substrates, respectively.

https://doi.org/10.1021/acs.macromol.5c00676
Macromolecules 2025, 58, 4138−4146

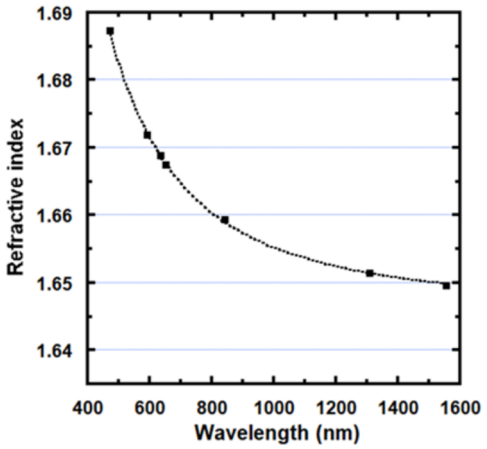

Figure 5. Wavelength dispersion of n_{av} values of the **Poly(BMMD/DTDO)** (entry 7) film determined by the prism coupler method.

anisotropy originating from the nearly free rotation around S−C bonds, as well as the presence of mixed exo/endo isomers in the main chains. Thus, introducing alicyclic units, a high content of sulfur element (calcd, 53.3%: obst, 52.6%), and sulfone groups (−SO_2−) into the main chain of a polymer is a promising strategy to obtain the optical films with high transparency, high n_{av}, high ν_d, and low Δn. Such balanced properties achieved in this study are visualized in the plots between n and ν of **Poly(BMMD/DTDO)** compared to those of BMMD-based PTESs and representative commercially available thermoplastic optical materials (Figure S23a), and the plots between n and T_g of BMMD-based PTESs (Figure S23b).

CONCLUSIONS

Herein, a novel alicyclic DT-based PTES was synthesized by the polyaddition of BMMD with DTDO. We succeeded in synthesizing and identifying DTDO with a boat-shaped conformation for the first time, as confirmed by NMR spectroscopy and X-ray crystallography. The model reaction between BM and DTDO afforded **BM2-DTDO**, a regioselective diadduct compound of BM to DTDO at 3-/5-positions, as confirmed by NMR spectroscopy and FD-MS measurements, supporting the mechanism of the Michael addition reaction. Based on this result, a high-molar-mass DT-based PTES, **Poly(BMMD/DTDO)**, with M_w values up to 23,900 g/mol was synthesized via the polyaddition reaction between BMMD and DTDO in the presence of DIPEA in NMP. The obtained **Poly(BMMD/DTDO)** showed high thermal stability as an aliphatic polymer, exhibiting a $T_d^{5\%}$ of 278 °C and high T_g of 131 °C. Furthermore, the **Poly(BMMD/DTDO)** film exhibited high transparency (T% = 94.7%@450 nm), a high n_{av} value (1.6719@594 nm) with a very small Δn value of −0.0002, and high ν_d^{TE}/ν_d^{TM} values of 37.8/37.6, which agreed well with the values obtained through TD-DFT calculations. Thus, a high composition of alicyclic structures, high sulfur contents (53.3 wt %), and incorporation of SO_2 units in a polymer result in a promising molecular design strategy for realizing balanced thermal and optical properties suitable for optical lens materials.

ASSOCIATED CONTENT

Supporting Information

The Supporting Information is available free of charge at https://pubs.acs.org/doi/10.1021/acs.macromol.5c00676.

Experimental sections; figures for ^{1}H, ^{13}C, FT-IR, and ^{1}H−^{1}H COSY NMR spectra, ORTEP diagram of DTDO, FD-MS spectrum, SEC UV traces, DSC thermogram, XRD pattern, calculated UV−vis absorption spectrum by DFT calculation, UV−vis absorption spectrum in DMSO, calculated wavelength dispersion of n_{av} values, plots for the relation between n and ν, and plots for the relation between n and T_g; scheme for synthetic routes; and tables for parameters determined by XRD analyses, polymerization results of BMMD and DT, and optical parameters; single-crystal X-ray crystallography (PDF)

Accession Codes

CCDC 2407849 contains the supplementary crystallographic data for this paper. These data can be obtained free of charge via www.ccdc.cam.ac.uk/data_request/cif or by emailing data_request@ccdc.cam.ac.uk or by contacting The Cambridge Crystallographic Data Centre, 12 Union Road, Cambridge CB2 1EZ, U.K.; fax: + 44 1223 336033.

AUTHOR INFORMATION

Corresponding Author

Tomoya Higashihara − *Department of Organic Materials Science, Graduate School of Organic Materials Science, Yamagata University, Yonezawa, Yamagata 992-8510, Japan*; orcid.org/0000-0003-2115-1281; Email: thigashihara@yz.yamagata-u.ac.jp

Authors

Keita Watanabe − *Department of Organic Materials Science, Graduate School of Organic Materials Science, Yamagata University, Yonezawa, Yamagata 992-8510, Japan*

Kazushi Enomoto − *RIKEN Center for Emergent Matter Science (CEMS), Wako, Saitama 351-0198, Japan*; orcid.org/0000-0002-5119-9043

Takumi Nagasawa − *HOYA Co, Akishima, Tokyo 196-8510, Japan*

Megumi Matsuda − *Department of Organic Materials Science, Graduate School of Organic Materials Science, Yamagata University, Yonezawa, Yamagata 992-8510, Japan*

Hiroshi Katagiri − *Department of Organic Materials Science, Graduate School of Organic Materials Science, Yamagata University, Yonezawa, Yamagata 992-8510, Japan*; orcid.org/0000-0003-4100-9995

Seigou Kawaguchi − *Department of Organic Materials Science, Graduate School of Organic Materials Science, Yamagata University, Yonezawa, Yamagata 992-8510, Japan*; orcid.org/0000-0002-5283-781X

Shinji Ando − *Department of Chemical Science and Engineering, Institute of Science Tokyo, Meguro-ku, Tokyo 152-8552, Japan*

Mitsuru Ueda − *Department of Organic Materials Science, Graduate School of Organic Materials Science, Yamagata University, Yonezawa, Yamagata 992-8510, Japan*

Complete contact information is available at: https://pubs.acs.org/10.1021/acs.macromol.5c00676

https://doi.org/10.1021/acs.macromol.5c00676
Macromolecules 2025, 58, 4138−4146

Author Contributions

Conceptualization: T.H. and M.U.; Methodology: K.W. and T.H.; Formal analysis and investigation: K.W. (synthesis and characterizations), K.E. (FT-IR calculation), T.N. (melting point measurement), M.M. (synthesis and characterizations), H.K. (X-ray crystallography), S.K. (optical characterizations), and S.A. (optical characterizations and calculations); Writing—original draft preparation: K.W. and T.H.; Writing—review and editing: T.H. and M.U.; Funding acquisition: T.H.; Supervision: T.H. All authors have contributed to reviewing the manuscript and given approval to its final version.

Funding

This work is mainly supported by HOYA corporation.

Notes

The authors declare no competing financial interest.

■ ACKNOWLEDGMENTS

The authors acknowledge Shigeru Matsuba at Yamagata University, Japan, for supporting the FD-MS measurement. The authors thank Prof. Hiroyuki Matsui at Yamagata University, Japan, for supporting the measurement of the polymer film thickness. The authors also thank Dr. Yuta Ito at Yamagata University, Japan, for operating the XRD experiment of the polymer film.

■ REFERENCES

(1) Dislich, H. Plastics as Optical Materials. *Angew. Chem., Int. Ed.* **1979**, *18* (1), 49−59.
(2) Krogman, K. C.; Druffel, T.; Sunkara, M. K. Anti-Reflective Optical Coatings Incorporating Nanoparticles. *Nanotechnology* **2005**, *16* (7), No. S338.
(3) Suwa, M.; Niwa, H.; Tomikawa, M. High Refractive Index Positive Tone Photo-Sensitive Coating. *J. Photopolym. Sci. Technol.* **2006**, *19* (2), 275−276.
(4) Jha, G. S.; Seshadri, G.; Mohan, A.; Khandal, R. K. Sulfur Containing Optical Plastics and Its Ophthalmic Lenses Applications. *e-Polymers* **2008**, *8* (1), No. 035.
(5) Liu, J. G.; Ueda, M. High Refractive Index Polymers: Fundamental Research and Practical Applications. *J. Mater. Chem.* **2009**, *19* (47), 8907−8919.
(6) Higashihara, T.; Ueda, M. Recent Progress in High Refractive Index Polymers. *Macromolecules* **2015**, *48* (7), 1915−1929.
(7) Buskens, P.; Burghoorn, M.; Mourad, M. C. D.; Vroon, Z. Antireflective Coatings for Glass and Transparent Polymers. *Langmuir* **2016**, *32* (27), 6781−6793.
(8) Riedel, D.; Wehlus, T.; Reusch, T. C. G.; Brabec, C. J. Polymer-Based Scattering Layers for Internal Light Extraction from Organic Light Emitting Diodes. *Org. Electron.* **2016**, *32*, 27−33.
(9) Salih, A. T.; Najim, A. A.; Muhi, M. A. H.; Gbashi, K. R. Single-Material Multilayer ZnS as Anti-Reflective Coating for Solar Cell Applications. *Opt. Commun.* **2017**, *388*, 84−89.
(10) Badur, T.; Dams, C.; Hampp, N. High Refractive Index Polymers by Design. *Macromolecules* **2018**, *51* (11), 4220−4228.
(11) Kleine, T. S.; Glass, R. S.; Lichtenberger, D. L.; Mackay, M. E.; Char, K.; Norwood, R. A.; Pyun, J. 100th Anniversary of Macromolecular Science Viewpoint: High Refractive Index Polymers from Elemental Sulfur for Infrared Thermal Imaging and Optics. *ACS Macro Lett.* **2020**, *9* (2), 245−259.
(12) Ma, H.; Jen, A. K. -Y.; Dalton, L. R. Polymer-Based Optical Waveguides: Materials, Processing, and Devices. *Adv. Mater.* **2022**, *14* (19), 1339−1365.
(13) Mazumder, K.; Voit, B.; Banerjee, S. Recent Progress in Sulfur-Containing High Refractive Index Polymers for Optical Applications. *ACS Omega* **2024**, *9* (6), 6253−6279.
(14) Scheiger, J. M.; Theato, P. High Refractive Index Sulfur-Containing Polymers (HRISPs). In *Sulfur-Containing Polymers: From Synthesis to Functional Materials*; WILEY-VCH GmbH, 2021, Chapter 9; pp 305−338.
(15) Jia, Y.; Shi, B.; Jin, J.; Li, J. High Refractive Index Polythiourethane Networks with High Mechanical Property *via* Thiol-Isocyanate Click Reaction. *Polymer* **2019**, *180*, No. 121746.
(16) Zhang, Y.; Wang, Y.; Chen, Y.; Yang, Z.; Chen, M.; Qin, Z. High-Refractive Index Polythiourethane Resin Based on 2,3-Bis((2-mercaptoethyl)thio)-1-propanethiol and 1,3-Bis(isocyanantomethyl)-cyclohexane Using Tertiary Amine Catalyst. *J. Appl. Polym. Sci.* **2021**, *138* (17), No. 50278.
(17) Puszka, A.; Sikora, J. W. Synthesis and Characterization of New Polycarbonate-Based Poly(thiourethane-urethane)s. *Polymers* **2022**, *14* (14), No. 2933.
(18) Seto, R.; Sato, T.; Kojima, T.; Hosokawa, K.; Koyama, Y.; Konishi, G. I.; Takata, T. 9,9′-Spirobifluorene-Containing Polycarbonates: Transparent Polymers with High Refractive Index and Low Birefringence. *J. Polym. Sci., Part A: Polym. Chem.* **2010**, *48* (16), 3658−3667.
(19) Liu, J. G.; Nakamura, Y.; Ogura, T.; Shibasaki, Y.; Ando, S.; Ueda, M. Optically Transparent Sulfur-Containing Polyimide− TiO_2 Nanocomposite Films with High Refractive Index and Negative Pattern Formation from Poly(amic acid)−TiO_2 Nanocomposite Film. *Chem. Mater.* **2008**, *20* (1), 273−281.
(20) Enomoto, K.; Kikuchi, M.; Narumi, A.; Kawaguchi, S. Surface Modifier-Free Organic−Inorganic Hybridization to Produce Optically Transparent and Highly Refractive Bulk Materials Composed of Epoxy Resins and ZrO_2 Nanoparticles. *ACS Appl. Mater. Interfaces* **2018**, *10* (16), 13985−13998.
(21) Watanabe, S.; Oyaizu, K. Methoxy-Substituted Phenylenesulfide Polymer with Excellent Dispersivity of TiO_2 Nanoparticles for Optical Application. *Bull. Chem. Soc. Jpn.* **2020**, *93* (11), 1287−1292.
(22) Watanabe, S.; Oyaizu, K. Catechol End-Capped Poly(arylene sulfide) as A High-Refractive-Index "TiO_2/ZrO_2-Nanodispersible" Polymer. *ACS Appl. Polym. Mater.* **2021**, *3* (9), 4495−4503.
(23) Mazumder, K.; Bittrich, E.; Voit, B.; Banerjee, S. Sulfur-Rich Polyimide/TiO_2 Hybrid Materials with A Tunable Refractive Index. *ACS Omega* **2023**, *8* (45), 43236−43242.
(24) Tawfilas, M.; Torres, G. B.; Lorenzi, R.; Saibene, M.; Mauri, M.; Simonutti, R. Transparent and High-Refractive-Index Titanium Dioxide/Thermoplastic Polyurethane Nanocomposites. *ACS Omega* **2024**, *9* (27), 29339−29349.
(25) Chemical Society of Japan *Chemical Handbook Basic II*; Maruzen: Tokyo, 1979; p 520.
(26) Okutsu, R.; Suzuki, Y.; Ando, S.; Ueda, M. Poly(thioether sulfone) with High Refractive Index and High Abbe's Number. *Macromolecules* **2008**, *41* (16), 6165−6168.
(27) Suzuki, Y.; Murakami, K.; Ando, S.; Higashihara, T.; Ueda, M. Synthesis and Characterization of Thianthrene-Based Poly(phenylene sulfide)s with High Refractive Index over 1.8. *J. Mater. Chem.* **2011**, *21* (39), 15727−15731.
(28) Kotaki, T.; Nishimura, N.; Ozawa, M.; Fujimori, A.; Muraoka, H.; Ogawa, S.; Korenaga, T.; Suzuki, E.; Oishi, Y.; Shibasaki, Y. Synthesis of Highly Refractive and Highly Fluorescent Rigid Cyanuryl Polyimines with Polycyclic Aromatic Hydrocarbon Pendants. *Polym. Chem.* **2016**, *7* (6), 1297−1308.
(29) Watanabe, S.; Oyaizu, K. Designing Ultrahigh-Refractive-Index Amorphous Poly(phenylene sulfide)s Based on Dense Intermolecular Hydrogen-Bond Networks. *Macromolecules* **2022**, *55* (6), 2252−2259.
(30) Watanabe, S.; Takayama, T.; Oyaizu, K. Transcending the Trade-Off in Refractive Index and Abbe Number for Highly Refractive Polymers: Synergistic Effect of Polarizable Skeletons and Robust Hydrogen Bonds. *ACS Polym. Au* **2022**, *2* (6), 458−466.
(31) Watanabe, S.; Nishio, H.; Takayama, T.; Oyaizu, K. Supramolecular Cross-Linking of Thiophenylene Polymers *via* Multiple Hydrogen Bonds toward High Refractive Index. *ACS Appl. Polym. Mater.* **2023**, *5* (4), 2307−2311.
(32) Watanabe, S.; Tsunekawa, Y.; Takayama, T.; Oyaizu, K. Diverse Side-Chain Transformation of High Refractive Index Methylthio-

https://doi.org/10.1021/acs.macromol.5c00676
Macromolecules 2025, 58, 4138−4146

Substituted Poly(phenylene sulfide)s. *Macromolecules* **2024**, *57* (6), 2897−2904.
(33) Suzuki, Y.; Higashihara, T.; Ando, S.; Ueda, M. Synthesis of High Refractive Index Poly(thioether sulfone)s with High Abbe's Number Derived from 2,5-Bis(sulfanylmethyl)-l,4-dithiane. *Polym. J.* **2009**, *41* (10), 860−865.
(34) Suzuki, Y.; Higashihara, T.; Ando, S.; Ueda, M. Synthesis and Characterization of High Refractive Index and High Abbe's Number Poly(thioether sulfone)s Based on Tricyclo[5.2. $1.0^{2,6}$]decane Moiety. *Macromolecules* **2012**, *45* (8), 3402−3408.
(35) Andrews, R. J.; Grulke, E. A. Glass Transition Temperatures of Polymers. In *Polymer Handbook*, 4th ed.; John Wiley & Sons, 1999; pp VI/193−VI/277.
(36) Howell, P. A.; Curtis, R. M.; Lipscomb, W. N. The Crystal and Molecular Structure of 1, 4-Dithiadiene. *Acta Crystallogr.* **1954**, *7* (6−7), 498−503.
(37) Parham, W. E.; Wynberg, H.; Ramp, F. L. Heterocyclic Vinyl Ethers. III. The Synthesis of 1,4-Dithiadiene and 1,4-Dithiadiene Disulfone. *J. Am. Chem. Soc.* **1953**, *75* (9), 2065−2069.
(38) Etkind, S. I.; Swager, T. M. The Properties, Synthesis, and Materials Applications of 1,4-Dithiins and Thianthrenes. *Synthesis* **2022**, *54* (22), 4843−4863.
(39) Peng, J.; Tian, T.; Xu, S.; Hu, R.; Tang, B. Z. Base-Assisted Polymerizations of Elemental Sulfur and Alkynones for Temperature-Controlled Synthesis of Polythiophenes or Poly(1,4-dithiin)s. *J. Am. Chem. Soc.* **2023**, *145* (51), 28204−28215.
(40) Grant, A. S.; Faraji-Dana, S.; Graham, E. A Convenient, One-Step Synthesis of 1,4-Dithiin. *J. Sulfur Chem.* **2009**, *30* (2), 135−136.
(41) Vessally, E. DFT Calculation on 1,4-Dithiin and S-oxygenated Derivatives. *Bull. Chem. Soc. Ethiop.* **2008**, *22* (3), 465−468.

https://doi.org/10.1021/acs.macromol.5c00676
Macromolecules 2025, 58, 4138−4146